I&EC research
Industrial & Engineering Chemistry Research

Article

pubs.acs.org/IECR

Probability-Based Design of Experiments for Batch Process Optimization with End-Point Specifications

Estefanía Colombo, Martin Luna, and Ernesto Martínez*

INGAR (CONICET-UTN), Avellaneda 3657, Santa Fe S3002 GJC, Argentina

Supporting Information

ABSTRACT: Consistently complying with end-point specifications, mainly end-use product properties, is a key issue to the competitiveness of batch processes. To maximize in some way the probability of observing successful runs, a series of experiments is specifically designed to pinpoint the smallest operating region that guarantees that end-point conditions can meet their desired targets. On the basis of data-driven modeling of the underlying binomial probability of success, the proposed methodology seeks to trade off improving parameter precision with experimenting in a reduced region where there is a high probability of satisfying end-point specifications. Two case studies are used to demonstrate the efficacy of the probability-based optimal design of experiments to find optimal policies for runs involving stochastic binary outcomes. Run-to-run improvement of the success rate for the operating policy in the acetoacetylation of pyrrole with diketene is first discussed. Results obtained for emulsion polymerization of styrene are also presented to illustrate how end-use properties, such as the tensile strength and melt index, can be maintained in their desired target regions by the proper choice of the operating policy.

1. INTRODUCTION

Most real-world optimization problems for batch processes are related to consistently complying with end-point specifications so as to minimize the variability in the product quality and process performance. For example, in many practical applications including foods, cosmetics, pharmaceuticals, etc., lipids are emulsified in an aqueous phase such that their end-use properties (rheological behavior, stability, color, etc.) completely define the values for an end user of the resulting products.[1] Emulsion polymerization processes are also representative examples of the importance of guaranteeing reproducibility and tight control of end-use properties such as the tensile strength and melt index by the proper choice of the operating policy.[2] With the advent of novel nanomaterials, the issue of controlling end-use properties fast became the main problem to be addressed in process development for reproducible manufacturing at the industrial scale.[3] For example, in tuning of the magnetic properties of iron oxide nanoparticles for biomedical applications, the quantitative effect of the size, shape, composition, and shell−core structure on the saturation magnetization, coercivity, blocking temperature, and relaxation time unambiguously defines a narrow range of operating conditions with high probability of success for repetitively obtaining the desired product.[4] Other novel processes where guaranteeing end-use properties is of paramount importance for the development of industrially scalable methods are the production of defect-free few-layer graphene by shear exfoliation in liquids[5] and the exfoliation and dispersion of layered materials by acoustic cavitation.[6] These are just representative examples of innovative processes for which the development of detailed first-principles models relating end-use properties to operating conditions is too costly in terms of time and/or money.

Proper settings of key process variables are critical for consistently complying with end-point specifications, including end-use product properties.[7−9] Searching for the optimal operating policy to guarantee that specifications for the process and/or product at the end of a run will be met with high probability is a stochastic optimization problem under uncertainty. A process is deemed as stochastic when runs carried out in the same operating conditions may yield different outcomes because of the effect of factors or inputs that cannot be controlled or manipulated. Ideally, a performance model for end-point conditions would be first established, and then the best settings can be searched offline via an optimization method. However, the performance in a run is only observed through a stochastic binary outcome—success or failure of the experiment—which is dependent on both the values for *controlled* inputs that define the process operating conditions and a number of uncontrolled (and possibly unknown) factors. As a result, the performance model is necessarily of a probabilistic nature and correlates the underlying binomial probability of success of an experiment with the alternative settings for controllable input factors.

The model-based design of dynamic experiments for optimal operation of batch processes has recently been addressed using active learning and Bayesian inference.[10−12] A decision-oriented design of experiments[13] takes into account how data obtained, and subsequently the model developed based on them, will be used in optimization and decision-making. To this aim, the focus of experimental design is not uncertainty reduction in parameter estimates or model discrimination but instead optimal decisions and process optimization. Accordingly, the information content of data obtained is of paramount importance because of the increasing need to reduce resources

Received: April 6, 2015
Revised: December 28, 2015
Accepted: January 15, 2016

DOI: 10.1021/acs.iecr.5b01295
Ind. Eng. Chem. Res. XXXX, XXX, XXX−XXX

required for achieving the specific objective or goal that the model builder is aiming at. Thus, simultaneous model identification and optimization[14,15] highlight a distinctive objective for the optimal design of dynamic experiments. However, modeling the probability of success over a region of interest (ROI) using first principles is a difficult undertaking for most batch processes and almost impossible for innovative products.[4] The main limitation for a first-principles model is that the impact of uncontrolled and unknown effects on the probability of success is difficult to account for using imperfect models and scarce data. If the model fails to represent these effects, its predictions may not be reliable enough for guaranteeing the desired end-point specifications. Therefore, an empirical, data-driven model that only relies on designed experiments and observations (success/failure) is the alternative of choice. The experimental design approach aims to get the maximum information from a given experimental effort. In most cases, a response surface model is built that summarizes and interpolates the process performance and provides a valuable guideline for improving operating conditions.

Fiordalis and Georgakis[16] have proposed a data-driven experimental design of dynamic experiments as a means of developing a response surface model that can be used to optimize complex batch processes for which it is difficult to develop a knowledge-driven model. Unfortunately, in their approach the probability of complying with end-point specifications is not explicitly modeled. To achieve this goal, it is necessary to develop a design of experiments that includes a compound criterion accounting for the dual purpose of obtaining efficient estimation parameters and simultaneuously maximizing the probability of a particular event. McGree et al.[17] have proposed different approaches for combining parameter estimation with opposing design criteria for nonlinear models. More specifically, McGree and Eccleston[18] have developed a probability-based optimal design that achieves such a trade-off by simultaneously optimizing a design with respect to the D-optimality criterion and, at the same time, maximizing a function of the probability of observing a desired outcome.

The search for a reduced region of operating conditions having a high probability of success can be formally stated as follows: given an input (parameter) space $\chi \subset \mathcal{R}$ and an unknown function $\pi:\chi \rightarrow [0,1]$, which represents the underlying binomial probability of success of an experiment, a short sequence of experiments should be generated such that an operating policy x^* having a high probability of success is found after a small number of runs. It is worth noting that, after each experiment, the only feedback received is a success or failure in complying with end-point specifications. To minimize costs, it is of main concern to also conduct most of the experiments in a reduced region of operating conditions where there is a higher probability of observing successes.

The optimization procedure should integrate an experimental design metric with a data-driven model of $\pi(x)$ to iteratively select the operating conditions for the next experiment to run. This gives rise to the need of a convenient trade-off between improving parametric precision in a response surface model for $\pi(x)$ and finding a reduced region of more successful operating policies. The ultimate goal of the optimization procedure is to recommend, after a rather small number of experiments, an operating policy x_r that minimizes the (typically unknown) error, or *simple regret*, $\max_{x\in\chi} \pi(x) - \pi(x_r)$, which is equivalent to $\max_{x_r\in\chi} \pi(x_r)$. To this aim, the sequence of runs should be generated so as to *exploit* what is already known to maximize the probability of success and, simultaneously, to *explore* the input space for efficient parameter estimation in modeling $\pi(x)$. Bias in data gathering should focus on improving the precision of parameters in $\pi(x)$ and assessing their effect on the binary response. A compound criterion for experimental design that addresses this issue is needed.

2. PROBABILITY-BASED OPTIMAL DESIGN

Data-driven modeling of the probability of success $\pi(x)$ typically resorts to generalized linear models (GLMs).[18,19] In regression modeling, GLMs extend the linear modeling framework to response variables that are not normally distributed and are constrained to a restricted range, so they are most commonly used to model binary or count data in classification problems. These models generalize linear regression by allowing the linear model to be related to the response variable via a link function.[20,21] Then, GLMs use a *response function* σ to convert a linear model with a range of $(-\infty, \infty)$ to an output that lies within $[0, 1]$ (i.e., a valid probability). Therefore, given a generalized regression model $\eta(x,\theta)$, the predicted success probability $\pi(x_i)$ at x_i is $\sigma[\eta(x_i,\theta)]$. The choice of θ for the latent linear regression model is typically accomplished via maximizing the likelihood of the data given the model. Thus, a GLM is used to describe the probability of success π of the experiment with regard to the operating conditions x_i using a given structure η with parameters θ.

For a given experimental design ξ consisting of the vectors of covariants $x_i \in X$, $\eta(x,\theta)$, for which the corresponding observations (responses) $\eta(x,\theta)$ have been obtained, GLMs are defined by three components: a distribution of the response, a linear predictor, and a link function $g(\bullet)$, which relates the mean of the response to the linear predictor. If the binary response variable has a Bernoulli distribution with success probability $\pi(x_i) = \sigma(y_i) = g^{-1}(y_i)$, a convenient link function is the logistic function:[19]

$$g(\pi) = \log\left(\frac{\pi}{1-\pi}\right) \tag{1}$$

To highlight the advantage of using eq 1, let us assume without any loss of generality that, for a given x_i, the binary response y_i follows the Bernoulli distribution.

The linear predictor used in this work has the following form:

$$\eta(\theta, \xi) = X\theta = a + bx_1 + cx_2 + dx_1x_2 + ex_1^2 + fx_2^2 \tag{2}$$

The likelihood for $y_i = 0$ and 1 is $L_i(\theta,y_i) = (\pi_i)^{y_i}(1-\pi_i)^{1-y_i}$, which, if the logistic link function is used, gives rise to $\log\left(\frac{\pi_i}{1-\pi_i}\right) = x_i\theta$, where π_i is the expectation of y_i, namely, the probability of success for x_i. Then, upon reordering, it can be stated that $\pi(\theta, \xi) = \frac{\exp(X\theta)}{1+\exp(X\theta)}$.

The aim of an optimum experimental design is to find a design ξ^* that maximizes a particular optimality criterion of interest. In this work, the goal is to generate a short sequence of runs whose outcomes for different operating policies help in the achievement of the dual goal of providing information about the model parameters θ and increasingly maximizing the probability of success π. To this aim, McGree and Eccleston[18] have proposed a compound criterion for experimental design

DOI: 10.1021/acs.iecr.5b01295
Ind. Eng. Chem. Res. XXXX, XXX, XXX−XXX

that balances two opposing criteria: D-optimality, which provides efficient estimates of the model parameters, and P-optimality, which maximizes the probability of observing a success.

D-optimality. A design ξ is said to be D-optimal if it maximizes $|\mathbf{M}(\theta,\xi)|$ or, equivalently, it minimizes $|\mathbf{M}^{-1}(\theta,\xi)|$. The Fisher information matrix is the inverse of the variance−covariance matrix of the maximum likelihood estimators of θ, and it indicates how well model parameters can be estimated by responses obtained through a design ξ. D-optimal designs therefore, in general, provide efficient estimates of the model parameters because they minimize the volume of ellipsoidal confidence regions around an estimate. For Bernoulli data with a logistic link function, the expected Fisher information matrix can be expressed as[18]

$$\mathbf{M}(\theta, \xi) = \mathbf{X}^{\mathrm{T}}\mathbf{W}\mathbf{X} \tag{3}$$

where the matrix $\mathbf{W}$ is $\mathrm{diag}[\pi_1(1-\pi_1),...,\pi_n(1-\pi_n)]$. The D-efficiency of any design ξ is defined with respect to the D-optimal design ξ_D^* as follows:

$$D_{\mathrm{eff}} = \left(\frac{|\mathbf{M}(\theta, \xi)|}{|\mathbf{M}(\theta, \xi_D^*)|}\right)^{1/q} \tag{4}$$

where q is the number of parameters in the response surface model $\pi(\theta,x)$.

P-optimality. This criterion maximizes the function of the probability of getting a specific outcome. In this work, the maximin criterion is specifically employed such taht the minimum probability of success is maximized, that is

$$\Phi^{(P)} = \min[\pi(\theta, \xi)] \tag{5}$$

where $\pi(\theta,x)$ is the probability of success of the design ξ and $\Phi^{(P)}$ is the objective function to be maximized, which represents the minimum value of the probability of success for experimental points in a given design ξ. Hence, the goal of P-optimality is to maximize the probability of success for the entry in the design ξ with the lowest probability of success. The P-efficiency of a given design ξ with respect to the P-optimal design ξ_P^* is defined as

$$P_{\mathrm{eff}} = \frac{\min[\pi_i(\theta, \xi)]}{\min[\pi_i(\theta, \xi_P^*)]} \tag{6}$$

Compound Criterion. The aim is to make a compromise between the two criteria described above, as the product of D- and P-efficiencies of an experimental design ξ, weighted by a mixing constant $0 \le \alpha \le 1$. That is[18]

$$\Phi^{(\mathrm{DP})} = [D_{\mathrm{eff}}(\xi)]^{\alpha}[P_{\mathrm{eff}}(\xi)]^{1-\alpha} \tag{7}$$

A mathematical program for the optimal design of experiments using the compound criterion can be stated as follows:

$$\max_{\xi} \Phi^{(\mathrm{DP})}(\xi) \tag{8a}$$

where

$$\log(\Phi^{(\mathrm{DP})}) = (\alpha/q)\log|\mathbf{M}(\theta, \xi)| + (1-\alpha)\log(\min[\pi_i(\theta, \xi_i)]), \quad \text{for } i = 1, \ldots, n \tag{8b}$$

$$\pi(\theta, \xi) = \frac{\exp(X\theta)}{1 + \exp(X\theta)} \tag{8c}$$

with bounds

$$\mathrm{LB}_w \le x_w \le \mathrm{UB}_w, \quad w = 1, \ldots, \dim(x) \tag{8d}$$

In this problem, the optimization variables are the experimental points (i.e., given values of the controlled variables) that comprise the design ξ (the model parameters θ are fixed while this optimization problem is solved).

3. OPTIMIZATION WITH STOCHASTIC BINARY OUTCOMES

On the basis of data-driven modeling of the underlying binomial probability of success and probability-based optimal design of experiments, a run-to-run optimization methodology is proposed to pinpoint a reduced region of operating conditions where there is a high probability of satisfying end-point specifications. When operating conditions are increasingly biased so as to increase the parametric precision for the response surface $\pi(\theta,x)$ toward the region where the probability of obtaining a desired outcome is high, a sequence of experiments is defined. The run-to-run optimization algorithm uses two nested loops, as shown in Figure 1.

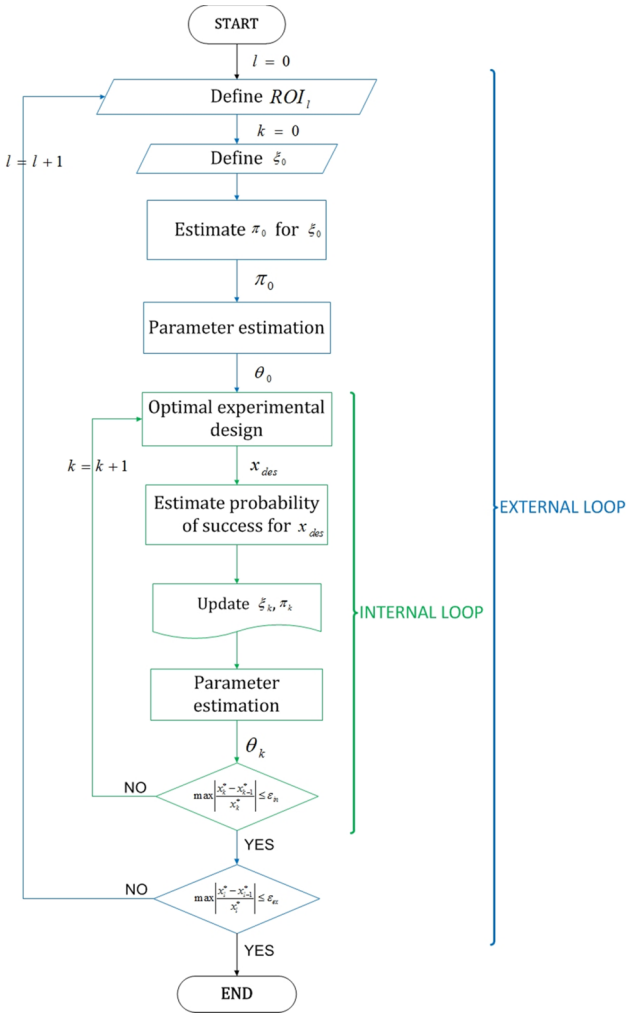

Figure 1. Run-to-run optimization using a probability-based optimal experimental design.

DOI: 10.1021/acs.iecr.5b01295
Ind. Eng. Chem. Res. XXXX, XXX, XXX−XXX

To begin with, the first step of the proposed approach consists of establishing the ROI for the process, that is, to establish the lower bounds LB and upper bounds UB for all input variables in the vector x. These bounds are defined by taking into account available data and prior knowledge about the process under study. Once these initial limits are defined, the algorithm starts with an external loop ($l = 0$) with a choice of points from a central composite design (CCD)[22] to decide where to experiment first in the ROI. Each design consists of a factorial design (the corners of a cube) together with center and star points that allow the estimation of second-order effects in the response surface of the success probability $\pi(\theta,x)$. For a full quadratic model with n input factors, CCDs have enough experimental points to estimate the $(n + 2)(n + 1)/2$ coefficients. For the sake of economy, only a fraction of points in the initial CCD are used for the each iteration of the external loop. At this stage, experimental points are chosen as follows: the center and star points are always chosen, whereas factorial points are randomly chosen up to a number necessary for parameter estimation. Because CCDs are orthogonal and rotatable, starting from a *fractional* CCD is a good way to minimize the prediction variance while comprehensively exploring the whole ROI. Later on in a case study, this choice for the initial experimental design is shown to be the most suitable option to start the external loop iterations of the run-to-run optimization methodology in Figure 1.

For any external loop iteration l, at each iteration of the internal loop (see Figure 1), an additional point corresponding to the current estimated optimum of the response surface model for the probability of success $\pi(\theta,x)$ is added to ξ_{k-1}. For the corresponding experimental design, ξ_k includes all data points from the first iteration ($k = 0$) up to the current iteration, and it is represented by

$$\xi_k = \begin{Bmatrix} x_{1,k} \\ x_{2,k} \\ \vdots \\ x_{n,k} \end{Bmatrix} \tag{9}$$

where $x_{i,k}$ is the ith experimental point added in the kth internal iteration.

For any point in ξ_k (for all experimental points in the initial design—external loop—and experimental points designed at every iteration of the internal loop), the probability of success is estimated using a number of replicas. That is, to calculate the probability of success in an experimental point, a number of experiments are needed (corresponding to the number r of specified replicas) for the same operating conditions. Then, the products obtained in each run are analyzed to determine whether the desired end-point specifications are satisfied. Accordingly, the probability of success in the experimental point is expressed as the percentage of runs where the batch meets its end-point specifications. As a result, the following vector for the success probabilities in the kth internal iteration is available:

$$\pi_k = \begin{Bmatrix} \pi_{1,k}(x_{1,k}) \\ \pi_{2,k}(x_{2,k}) \\ \vdots \\ \pi_{n,k}(x_{i,k}) \end{Bmatrix} \tag{10}$$

Using vectors ξ_k and π_k, the response surface of the probability of success is modeled as a GLM with the logistic function as the link function. The corresponding vector of model parameters for the kth internal iteration is denoted by θ_k. Accordingly, the model for the probability of success over the ROI for the lth iteration of the external loop is

$$\pi_k = \frac{\exp[\eta(\theta_k, x)]}{1 + \exp[\eta(\theta_k, x)]}, \quad x \in \text{ROI} \tag{11}$$

Using the model in eq 11 with θ_{k-1} from the previous iteration, in the kth internal iteration, a new experimental point x_{des} is added by solving the mathematical program in eq 8 using the compound objective previously described in eq 7, where the current design is defined by $\xi_k = [\xi_{k-1}, x_{\text{des}}]$. As soon as the probability of success at x_{des} is estimated by doing a number of experimental replicas, vectors ξ_k and π_k are updated and a new vector of model parameters θ_k is obtained. Later on, the predicted optimum x_k* that maximizes the success probability is obtained and compared with the one from the previous iteration to check convergence of the internal loop using the following stopping criterion:

$$\max \left| \frac{x_k^* - x_{k-1}^*}{x_k^*} \right| \leq \varepsilon_{\text{in}} \tag{12}$$

When the internal stopping condition is satisfied, the optimum for the current iteration of the external loop is calculated as $x_l^* = x_k^*$, and the stopping condition for the external loop is checked using the criterion

$$\max \left| \frac{x_l^* - x_{l-1}^*}{x_l^*} \right| \leq \varepsilon_{\text{ex}} \tag{13}$$

For obtaining the maximum of the response surface model of the probability of success $\pi(\theta_k,x)$, the following mathematical program is solved in the kth internal iteration

$$\max_x \pi(\theta_k, x)$$
$$\text{LB}_w^l \leq x_w \leq \text{UB}_w^l, \quad w = 1, \ldots, \dim(x) \tag{14}$$

where LB_w^l and UB_w^l are the lower and upper bounds of the wth explanatory variable in the lth iteration of the external loop.

Whenever the external stopping criterion in eq 12 is not fulfilled, the run-to-run strategy begins a new iteration of the external loop, but now the ROI_l is reduced to a fraction (say a quarter) of the one in the previous iteration centered at the optimum x_{l-1}* but always included in the initial ROI. If the optimum is on one boundary of the initial ROI or near it, the new ROI_l is conveniently defined so as to be within the initial ROI and with a center that is the closest to x_{l-1}*. In this work, the bounds LB_w^l and UB_w^l in each iteration of the external loop are defined as follows:

For $l = 1$, define LB_w^l and UB_w^l based on the literature or previous experience in the process.

For $l \geq 2$, define the current ROI_l as a quarter of ROI_{l-1} with the center at x_{l-1}*.

Every time a new external iteration begins with a reduced ROI, the first internal iteration begins with fractional CCD based on the ROI_l. Additional iterations in the internal loop increasingly add new experimental points using probability-based optimal design (see eq 8). When both loops converge, the last optimal point obtained is considered to be the optimal operating point of the process to work with a high probability

DOI: 10.1021/acs.iecr.5b01295
Ind. Eng. Chem. Res. XXXX, XXX, XXX−XXX

of complying with end-point specifications, e.g., end-use properties of the obtained product.

An alternative to deciding when to stop iterating in any of the loops is to set a maximum number of iterations. On the one hand, defining a maximum number of iterations in the external loop prevents the search for an optimal point within a ROI_l that is too small, bearing in mind the intrinsic process variability. On the other hand, defining a maximum number of iterations for the internal loop prevents too much experimentation in operating conditions that are very close to each other so that they bring almost the same information about the process optimum and do not improve significantly the parametric precision for the response surface model of the probability of success.

4. CASE STUDIES

4.1. Acetoacetylation of Pyrrole with Diketene. The first representative case study to be considered is the acetoacetylation of pyrrole with diketene, for which Ruppen et al.[23] have proposed the following set of reactions:

$$P + D \xrightarrow{k_A} PAA$$

$$D + D \xrightarrow{k_D} DHA$$

$$D \xrightarrow{k_O} \text{oligimers}$$

$$PAA + D \xrightarrow{k_F} F$$

where P, D, PAA, and DHA stands for pyrrole, diketene, 2-acetoacetylpyrrole, and dehydroacetic acid, whereas F is a byproduct. The corresponding rate laws for the set of reactions above are

$$r_{PAA} = k_A C_D C_P$$

$$r_{DHA} = k_D C_D^{\,2}$$

$$r_O = k_O C_D$$

$$r_F = k_F C_{PAA} C_D$$

The nominal values of the kinetic parameters given elsewhere[23] are as follows: k_A° = 0.53 L/(mol·min), k_D° = 0.128 L/(mol·min), k_O° = 0.028 min^{-1}, and k_F° = 0.001 L/(mol·min). The process is conducted in a semibatch isothermal reactor, where a solution of diketene was added at a constant feed flow for a specified feed time. A first-principles model for the acetoacetylation process[23] is given in the Supporting Information.

To test the proposed optimization approach, a probabilistic model of the semibatch reactor to be used as an in silico proxy for carrying out experimentation is now described. Following Ruppen et al.,[23] who stated that the value of k_F could be set to 0.001 min^{-1} (because this was the largest value encountered in all experiments and was thus established as an upper bound), the probabilistic effect on end-point conditions was incorporated by superimposing a random variability term over their nominal values in the other three kinetic parameters of the simulation model as follows:

$$k_A = k_A^\circ \pm \frac{SP}{2 \times 100}$$

$$k_D = k_D^\circ \pm \frac{SP}{2 \times 100}$$

$$k_O = k_O^\circ \pm \frac{SP}{2 \times 100} \quad (15)$$

where SP is the percentage of variability considered for the values of the kinetic constants. Note that, in eq 15, the interval over which each parameter is defined has been centered in its corresponding nominal value. It is worth highlighting that the model is only used to generate experimental data, and it is not available to the user of the proposed methodology. The values of the kinetic constants and their variability are unknown as well.

For run-to-run optimization of the probability of success, the input variables are the feed flow rate to the reactor (in liters per minute) and the feeding time period for the diketene (in minutes). To this aim, a dynamic optimization problem must be solved, where the policy is a time-varying feeding profile that consists of two parameters. To comply with the specifications at the end of the run, it is necessary to find the optimal setting of these parameters. Figure 2 graphically shows the considered profile with the parameters used for maximizing the probability of success. To begin with, the feeding profile is parametrized in this way in order to analyze the results obtained in an easier and graphical way. Later on, an analysis of the same case study is made but considering a more flexible profile defined by four parameters to be optimized. The response variables are the concentrations of different species (in moles per liter) in the reactor at the end of each run. To comply with end-point specifications, these concentrations of reagents and products should be maintained within certain desired values. More specifically, for productivity and safety, the concentrations at the final time of each run should be verified:

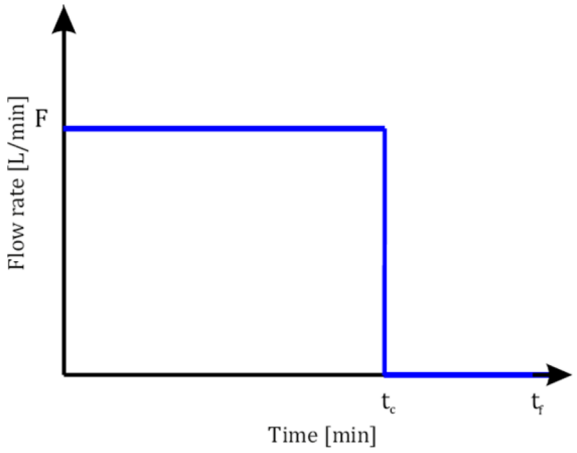

Figure 2. Feeding profile for diketene defined by two parameters. The final time is assumed to be fixed.

$$C_{PAA}(t_f)\, \nu_R(t_f) \geq 0.46 \text{ mol}$$

$$C_{DHA}(t_f) \leq 0.15 \text{ mol/L}$$

$$C_D(t_f) \leq 0.025 \text{ mol/L}$$

To implement the run-to-run optimization methodology, it is necessary to define first the following set of hyperparameters:

DOI: 10.1021/acs.iecr.5b01295
Ind. Eng. Chem. Res. XXXX, XXX, XXX−XXX

lower and upper operating bounds of each input variable (LB and UB), number of designed experimental points in each internal loop iteration (ep), number of replicates to perform in each experimental point (r), maximum number of internal loops (il), maximum number of external loops (el), and internal and external stop criteria (ε_{in} and ε_{ex}). The values chosen for hyperparameters for this case study are shown in Table 1.

Table 1. Hyperparameter Values for the Acetoacetylation of Pyrrole with Diketene

parameter	value
LB	$[150, 0.9 \times 10^{-3}]$
UB	$[235, 1.5 \times 10^{-3}]$
ep	1
r	10
il	6
el	4
ε_{in}	0.5×10^{-2}
ε_{ex}	1×10^{-3}

A maximum number of six iterations for the internal loop help to prevent too many points being put in a too small a ROI, which would imply getting little information at the expense of costly experimentation. Also, a maximum of four iterations for the external loop are used to avoid narrowing of the ROI unnecessarily bearing the intrinsic variability of the process.

The values of SP used to simulate the intrinsic process variability were 5%, 10%, and 20%. Figure 3 depicts the contour levels of the response surface models obtained for the chosen values of SP and within the boundaries of the same initial ROI. As can be seen, there exists a zone with a high probability of obtaining the desired end-point specifications whose size depends on the chosen level of variability. This is the target reduced ROI that the proposed run-to-run methodology will hopefully find using the outcomes of experimental runs only.

To assess its performance in the acetoacetylation process, the proposed methodology was implemented, and the results obtained until convergence of the external loop are given using SP = 10% and α = 0.25. Figure 4 depicts the successive reduction of the ROI as external iterations are carried out and the experimental points are tried by the methodology. As can be seen in this particular trial, there exists a successive reduction of the initial ROI toward a small set of operating conditions with a high probability of success. The results of this specific trial are presented in Table 2, which provides for each external loop bounds for the reduced ROI obtained, the optimal operating policy, and the number of experimental points required to complete the external loop. After the last iteration of the external loop, a very small ROI with high probability of success is obtained. The optimal operating policy corresponds to a feed time of 205.26 min and a feed rate of 1.1×10^{-3} mol/s. This optimal policy has a probability of success of 100.00% and requires a total of 35 experimental points to be found.

To assess the sensitivity of the proposed run-to-run approach, the present case study is solved using α = 0.25 and considering the three alternative values of SP previously mentioned. The influence of the mixing constant α in the optimization strategy of Figure 1 was analyzed a priori in order to choose the optimal value for this parameter; a summary of the results obtained is given in the Supporting Information, where it is demonstrated that α = 0.25 is the best value for this parameter.

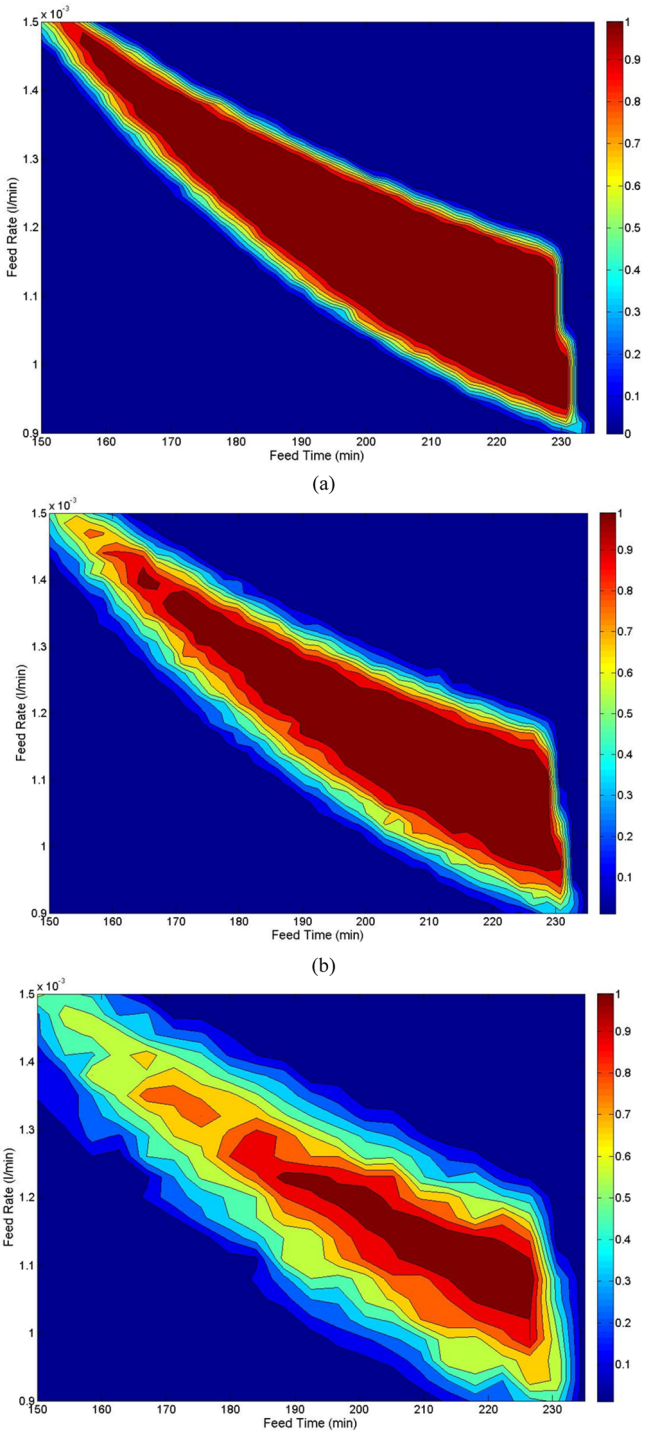

Figure 3. Probability of success over the initial ROI for the acetoacetylation of pyrrole with diketene using the feeding profile in Figure 2 with SP = (a) 5%, (b) 10%, and (c) 20%.

Choosing the same hyperparameters and starting from the same initial ROI, the sequential experimental design methodology in Figure 1 has been implemented until convergence in 100 independent trials for each value of SP previously considered. Because the in silico simulation model used is of a stochastic nature, the outcome in each operating condition may vary, and therefore the proposed methodology may lead to different solutions in each trial. It is worth remembering that by

DOI: 10.1021/acs.iecr.5b01295
Ind. Eng. Chem. Res. XXXX, XXX, XXX−XXX

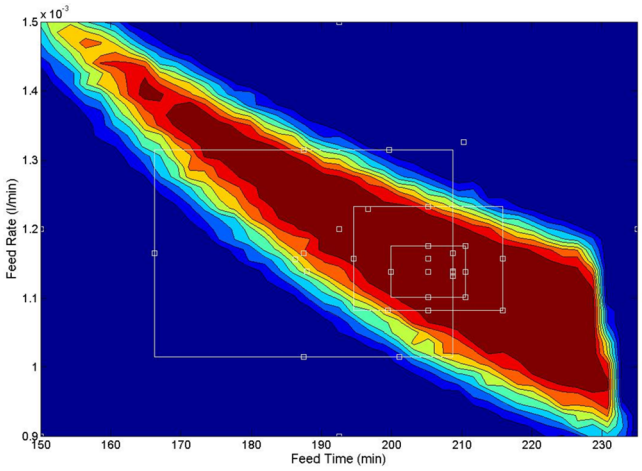

Figure 4. Complete trial (until convergence of both loops) of the run-to-run optimization methodology in Figure 1 for the acetoacetylation of pyrrole with diketene (SP = 10%; α = 0.25) using the feeding profile in Figure 2.

a trial we refer to a full implementation of the algorithm until convergence. Then, in each one of these independent trials, a different optimum operating policy is found. The results obtained are shown in Table 3, where the percentages of all trials of the methodology (based in the 100 independent implementations) that find an operating policy that complies with the end-point specifications, for different levels of success, are given. This analysis has been performed for three different values of SP: 5%, 10%, and 20%.

Table 3 includes analysis of 100 independent trials of the methodology with an exceedingly high process variability (SP = 20%); although unlikely in the process industry, this significantly high level of intrinsic variability is only used here to demonstrate the outstanding capability of the proposed approach. The resulting reduced ROI defines an optimum operating policy that guarantees a probability of success of 95% for 39% of the trials made. Despite the exceedingly high intrinsic variability, the obtained optimal policy has a probability of success above 80% in most of the runs (97%). Moreover, only 3% of all trials fall into a region with a probability of success of less than 80%, whereas all trials made achieved a region where the probability of success is higher than 60%. It is worth noting that, within the initial ROI (see Figure 3c), only a small part of it (near 9.75%) has a probability of success of over 80%. Despite this, the methodology in Figure 1 was able to find a reduced region of operating conditions with a high probability of success in most of the trials.

The sensitivity of the results obtained for different initial experimental designs ξ_0 is now analyzed. Bearing in mind that the operating policy has two input variables, a minimum of six experimental points are required to begin any external loop

Table 3. Percentage of Trials That Found an Operating Policy That Complies with the End-Point Specifications for Different Levels of Success and Different Values of SP Using the Feeding Profile in Figure 2 and α = 0.25

minimum probability of success required (%)	percentage of runs that reach the desired reduced ROI (%)		
	SP = 5%	SP = 10%	SP = 20%
95	100	100	39
90	100	100	75
85	100	100	87
80	100	100	97
70	100	100	99
60	100	100	100

iteration. The initial designs analyzed were a fractional CCD (see Figure 5a), a factorial design plus one point in the center and one point in the middle of one of the boundaries, and finally six randomly chosen points scattered within the boundaries of the ROI. These three alternative designs are shown graphically in Figure 5. Figure 6 depicts the evolution of the methodology depending on the initial design chosen. To favor doing a fair, yet simple comparison, results obtained are only shown for each ξ_0 until completion of the first external loop, namely, until the first reduction of the initial ROI is done. Different graphs in Figure 6 highlight the initial ROI, the initial design points, points that are added by the optimization methodology, and the resulting ROI reduction after convergence of the external loop. Successive response surfaces that are found with the addition of new optimally designed points added within the internal loop are provided in the Supporting Information. From Figure 6, it seems that the best alternative is to start each iteration of the external loop with a CCD, which ensures an appropriate reduction of the initial ROI with fewer experimental points.

To highlight the issue of the optimal design of a dynamic experiment, let us consider a more elaborate feeding profile having four variables to be optimized. As is shown in Figure 7, the input variables now are the initial feed flow rate to reactor (F_1), the switching time (t_s), the value of the feed flow rate after the switching time (F_2), and the overall feeding time period for diketene (t_c). Once again, the final reaction time (t_f) is fixed, and the response variables are the concentrations of the different species at the end of each run, whereas the end-point specifications are the same for this case study.

For each value of the parameter SP considered, 100 independent trials were performed and an optimum operating policy was found in each one of these trials. In Table 4, the results obtained for different levels of the process intrinsic variability simulated are shown.

As can be seen, when the intrinsic process variability is rather low (SP = 5%) or even significant (SP = 10%), the proposed

Table 2. Summary of the Results of the Trial Depicted in Figure 4 (SP = 10% and α = 0.25) Using the Feeding Profile in Figure 2

external loop	lower bound feed time (min)	upper bound feed time (min)	lower bound feed rate (mol/s)	upper bound feed rate (mol/s)	optimal feed time (min)	optimal feed rate (mol/s)	probability of success	total experimental points required
1	150.00	235.00	0.9×10^{-3}	1.5×10^{-3}	187.48	1.2×10^{-3}	0.9300	8
2	166.23	208.73	1.05×10^{-3}	1.35×10^{-3}	205.25	1.2×10^{-3}	0.9900	12
3	194.63	215.88	1.03×10^{-3}	1.18×10^{-3}	205.26	1.1×10^{-3}	0.9900	8
4	199.95	210.57	1.06×10^{-3}	1.14×10^{-3}	205.26	1.1×10^{-3}	1.0000	7

DOI: 10.1021/acs.iecr.5b01295
Ind. Eng. Chem. Res. XXXX, XXX, XXX−XXX

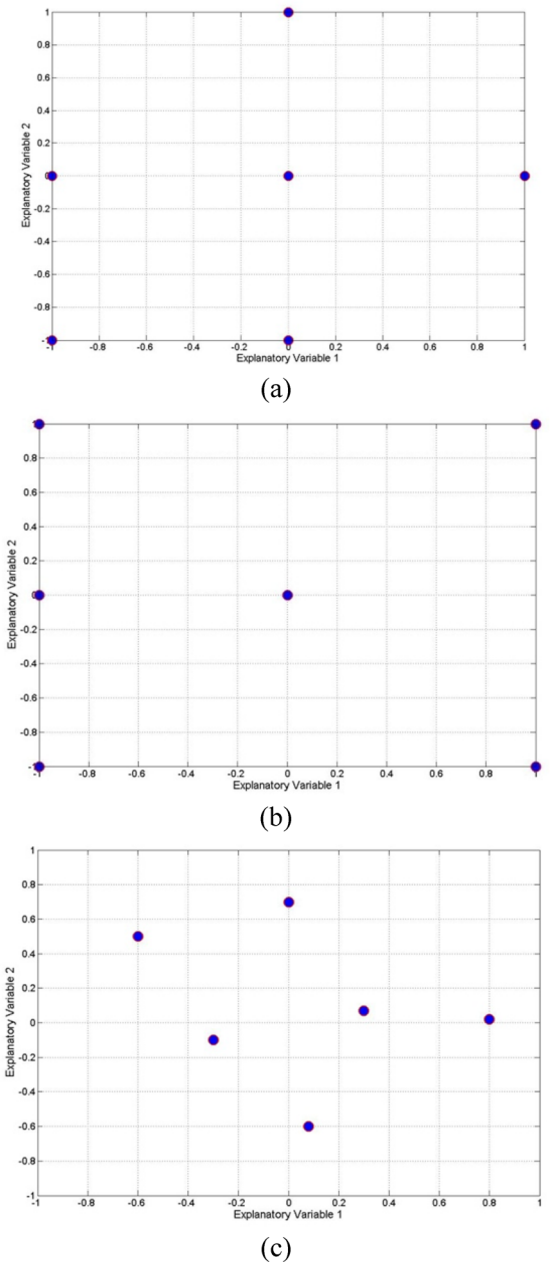

Figure 5. Initial designs used for internal loop iterations: (a) fractional CCD; (b) factorial design plus one point in the center and one point in the middle of one of the boundaries; (c) six randomly chosen points scattered within the ROI.

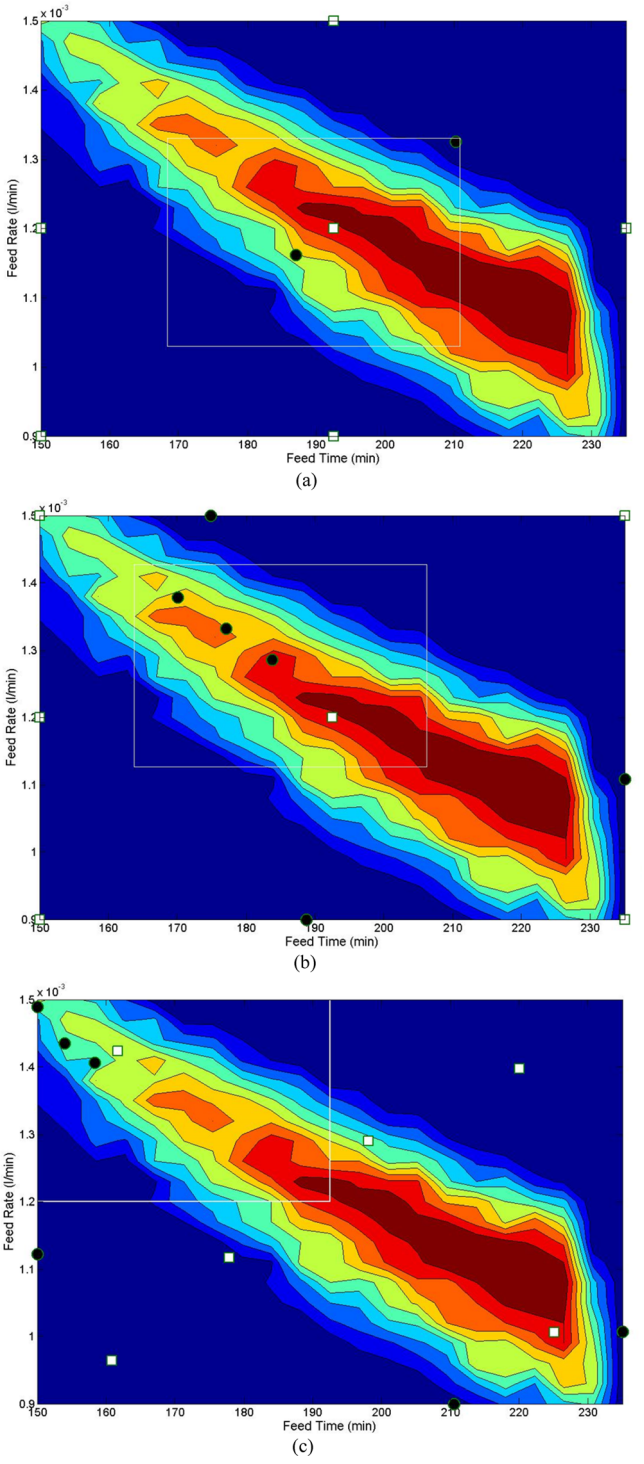

Figure 6. Evolution of the ROI after the first iteration of the external loop for different initial designs (white squares correspond to the initial design points, whereas black circles are points added during internal loop iterations): (a) fractional CCD with one point in one of the boundaries; (b) factorial design adding one point in the center and one point in the middle of one boundary; (c) six randomly chosen points scattered within the ROI.

methodology can find a reduced region of operating conditions having a high probability of success for most of the trials. More specifically, all trials end up in a zone with a probability over 95% of meeting end-point specifications. As can be expected, because the process variability is exceedingly high (SP = 20%), it is a bit more difficult to find a reduced region with a probability of success of ca. 100% for all trials. Despite this, the proposed method still locates a reduced ROI such that the optimal feeding profile is successful in a high percentage of trials. As a result, it was demonstrated that the methodology in Figure 1 can be used to optimize a time-varying profile. It is fair to acknowledge, though, that, as the number of parameters increases, the experimental effort required will also increase, as is also the case with response surface methods. However, using the proposed approach, the magnitude of such an increase will depend on the intrinsic process variability. For higher levels of variability, more replicas for the same operating policy are needed, hence higher costs.

DOI: 10.1021/acs.iecr.5b01295
Ind. Eng. Chem. Res. XXXX, XXX, XXX−XXX

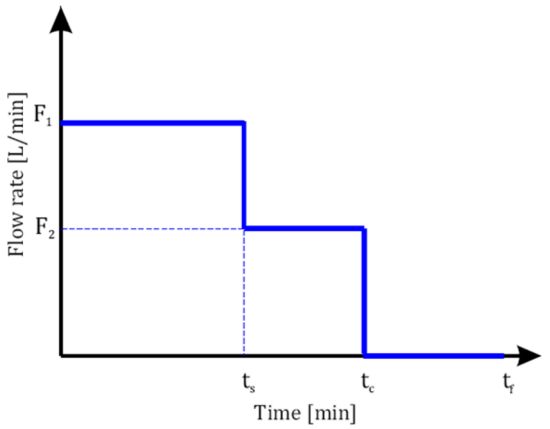

Figure 7. Feeding profile for diketene defined by four parameters. The final time is assumed to be fixed.

Table 4. Percentage of Trials That Found an Operating Policy That Complies with the End-Point Specifications for Different Levels of Success and Different Values of SP Using the Feeding Profile in Figure 7

minimum probability of success required (%)	percentage of runs that reach the desired reduced ROI (%)		
	SP = 5%	SP = 10%	SP = 20%
95	100	100	87
90	100	100	90
85	100	100	91
80	100	100	91
70	100	100	95
60	100	100	96

4.2. Emulsion Polymerization of Styrene. As a very representative example of a process where complying with end-use product properties is mandatory, emulsion polymerization of styrene is now addressed. Mathematical models for this process have been discussed in Liotta et al.[24] and Li and Brooks[25] as well as in more recent works.[26−28] Similarly to the first case study, a probabilistic simulation model of the process is used to describe the effect of the intrinsic variability and modeling errors in end-point specifications. A random variability effect using SP = 10% in the process dynamics is added to the initial amounts of each population of seeded particles as follows:

$$N_1 = 20 \times 10^{17} \pm \frac{SP}{2 \times 100}$$
$$N_2 = 80 \times 10^{17} \pm \frac{SP}{2 \times 100}$$
$$N_3 = 20 \times 10^{17} \pm \frac{SP}{2 \times 100} \quad (16)$$

The kinetic model and conservation equation for the process accounts for the following key variables: volume balance for the reaction medium, volume balance of particles in each population, molar balance of the monomer, balance of the average number of radicals per particle for each population, polymerization rate for each population, addition rate of the chain-transfer agent (CTA), molar balance of the initiator, and molar balance for the CTA. All constitutive equations and balances that made up the dynamic model have been developed in previous works, and only a summary of them is provided in the Supporting Information. Again, this in silico model and the variability of the particles' size are assumed to be unknown to the user of the proposed approach and are only used here to generate data in order to test the proposed methodology.

In this case study, it is of special concern that the final product obtained satisfies two end-use properties: melt flow index (MI) and tensile strength (σ). These properties may be reliably estimated using correlations that are dependent on the weight-average molecular weight (MW_w) and number-average molecular weight (MW_n), respectively:[2]

$$MI = \frac{30}{MW_w^{3.4} \times 10^{-18} - 0.2} \quad (17)$$

$$\sigma = 7390 - 4.51 \times 10^8 \left(\frac{1}{MW_n}\right) \quad (18)$$

where MW_w and MW_n can be calculated by[2,27,29]

$$MW_w = \frac{\sum_{i=0}^{n_p} \lambda_i^2 + \sum_{i=0}^{n_p} \mu_i^2}{\sum_{i=0}^{n_p} \lambda_i^1 + \sum_{i=0}^{n_p} \mu_i^1} \quad (19)$$

$$MW_n = \frac{\sum_{i=0}^{n_p} \lambda_i^1 + \sum_{i=0}^{n_p} \mu_i^1}{\sum_{i=0}^{n_p} \lambda_i^0 + \sum_{i=0}^{n_p} \mu_i^0} \quad (20)$$

where λ_i^j is the jth moment of the *live* polymer chain for species i and μ_i^j is the jth moment of the *dead* polymer chain for species i. The balances of the moments for the live and dead polymers are available in the Supporting Information.

To apply the run-to-run optimization methodology in Figure 1, the monomer and CTA feed rates to the polymerization reactor, both of them in moles per seconds, were chosen as input variables to guarantee end-use properties of the resulting product stated as follows:

$$1.25 \times 10^{-4} < MI\ [g/min] \leq 7.5 \times 10^{-4}$$
$$6900 < \sigma\ [psi] \leq 7200$$

The values of the hyperparameters used to implement the proposed optimization methodology in this case study are given in Table 5.

Table 5. Hyperparameter Values for Emulsion Polymerization of Styrene

parameter	value
LB	$[0.0184, 1 \times 10^{-4}]$
UB	$[0.026, 8 \times 10^{-4}]$
ep	1
r	10
il	6
el	4
ε_{in}	0.5×10^{-2}
ε_{ex}	1×10^{-3}

To evaluate the proposed run-to-run approach for finding a reduced ROI having a high probability of success, the polymerization of styrene is now addressed. This case study constitutes a challenging problem for the proposed methodology in Figure 1. Figure 8 depicts the contour levels of the response surface models for the probability of success obtained for the initial ROI chosen.

DOI: 10.1021/acs.iecr.5b01295
Ind. Eng. Chem. Res. XXXX, XXX, XXX−XXX

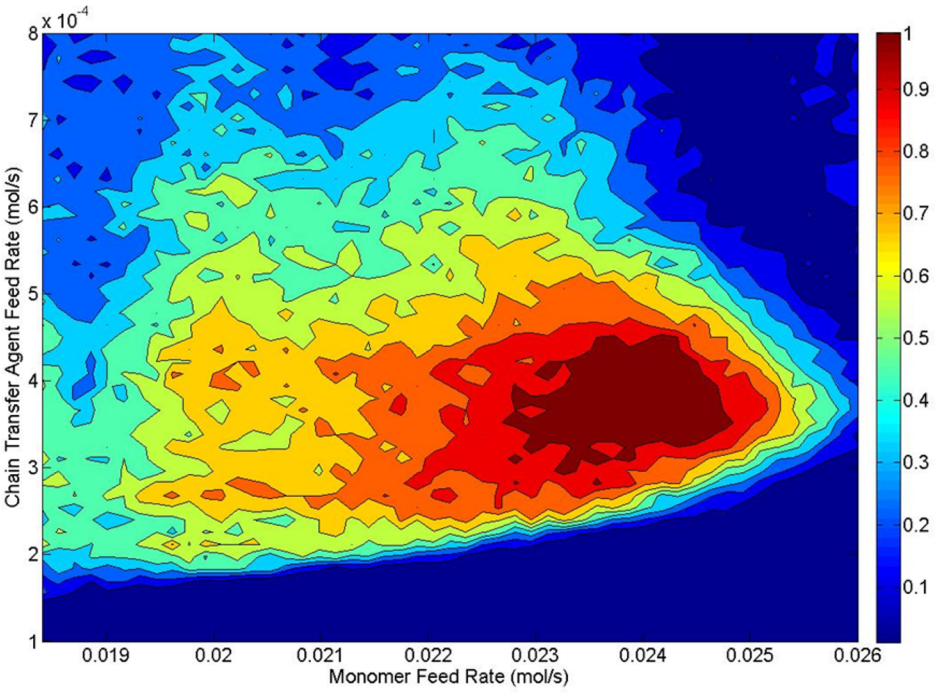

Figure 8. Probability of success over the initial ROI for emulsion polymerization of styrene with SP = 10%.

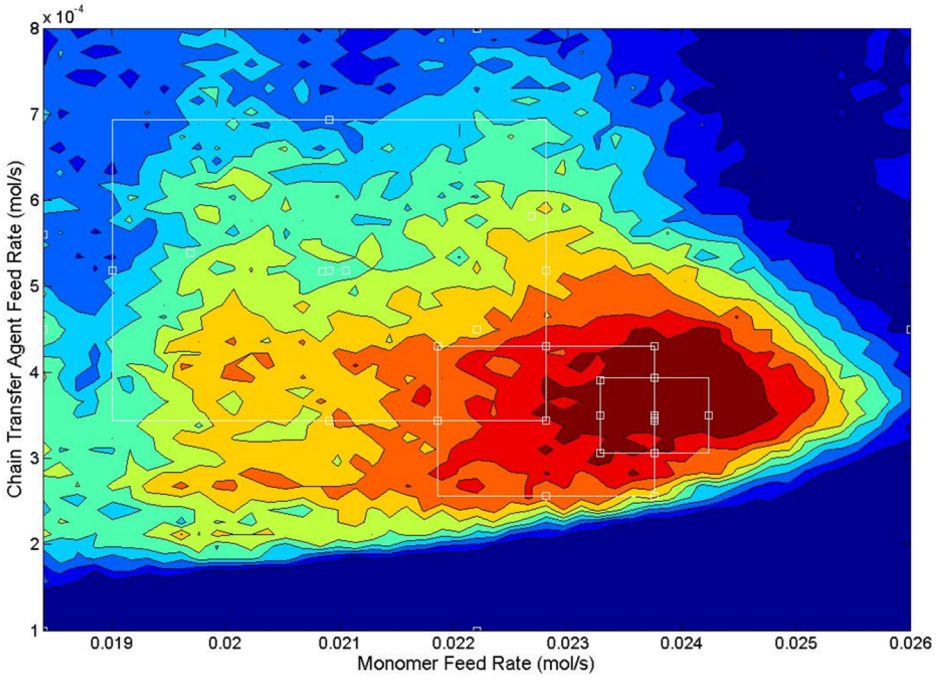

Figure 9. Complete trial (until the convergence of both loops) of the run-to-run optimization methodology in Figure 1 for emulsion polymerization of styrene (SP = 10% and α = 0.25).

Table 6. Summary of the Results of the Trial Depicted in Figure 9 (SP = 10% and α = 0.25)

external loop	lower bound monomer feed rate (mol/s)	upper bound monomer feed rate (mol/s)	lower bound CTA feed rate (mol/s)	upper bound CTA feed rate (mol/s)	optimal monomer feed rate (mol/s)	optimal CTA feed rate (mol/s)	probability of success	total experimental points required
1	0.0184	0.0260	1×10^{-4}	8×10^{-4}	0.0209	5×10^{-4}	0.5100	10
2	0.0190	0.0228	3.25×10^{-4}	6.75×10^{-4}	0.0228	3×10^{-4}	0.8400	9
3	0.0219	0.0238	2.13×10^{-4}	3.88×10^{-4}	0.0238	4×10^{-4}	0.9300	9
4	0.0233	0.0243	3.56×10^{-4}	4.44×10^{-4}	0.0242	4×10^{-4}	0.9700	7

DOI: 10.1021/acs.iecr.5b01295
Ind. Eng. Chem. Res. XXXX, XXX, XXX−XXX

Figure 9 depicts, for a given trial, the systematic reduction of the ROI as external loop iterations in the proposed methodology in Figure 1 are carried out. Table 6 provides a summary of the results obtained, including upper/lower bounds for the reduced ROI for external loop iterations. Accordingly, to maximize the probability of success, the monomer feed rate should lie in the interval of 0.0233−0.243 mol/s, whereas the CTA feed rate must be between 3.56×10^{-4} and 4.44×10^{-4} mol/s. The optimal operating policy corresponds to a monomer feed rate of 0.0242 mol/s and a CTA feed rate of 4×10^{-4} mol/s. The probability of success for this optimal policy is 97%, whereas the total number of experimental points required to obtain this optimal policy was of 35.

On the basis of 100 independent trials of the run-to-run optimization strategy, the probability of success of the resulting optimal policy for different degrees of confidence is highlighted in Table 7. The results obtained demonstrated that when the proposed methodology is used, the optimal policy found has a probability of success of more than 90% in 47% of the trials. Moreover, the obtained optimal has a probability of success higher than 80% in 73% of the trials. Finally, only 7% of the trials provide an optimal policy with a probability of success of less than 60%.

Table 7. Percentage of Trials That Found an Operating Policy That Complies with the End-Point Specifications for Different Levels of Success (SP = 10% and α = 0.25)

minimum probability of success required (%)	percentage of trials that reach a zone with a given level of success (%)
95	15
90	47
85	61
80	73
70	86
60	93

With implementation of this second case study, it was possible to demonstrate that by embedding data-driven modeling of the probability of success in the proposed run-to-run optimization approach it is feasible to find a reduced ROI where end-use properties can be guaranteed with high probability. The results obtained prove that, for complex processes where there are no reliable models for policy optimization, the proposed methodology is an appealing tool to obtain the desired operating region by performing only a small number of experiments.

5. CONCLUDING REMARKS

The usefulness of the probability-based design of experiments for batch process optimization with end-point specifications has been proposed as a way to define an optimal operating policy with a high probability of obtaining the desired outcome. The proposed methodology is data-driven, which makes it very appealing for innovative processes for whom first-principles knowledge or detailed models are not available. The methodology resorts to a compound criterion for optimal experimental design in order to balance parametric precision with the probability of success. As a result, the optimization strategy in Figure 1 increasingly biases operating conditions toward a reduced region of operation with higher success probabilities, while the response surface model is improved. In the limit, as the number of iterations for the external loop increases, the proposed method will always converge toward a target region of operating conditions within the initial ROI, where the probability of success is the highest. Should there be more than one reduced ROI having equally high success probabilities, the method will find only one of them. In such a case, because of the bias introduced through the initial approximation of the success probability response surface, it cannot be guaranteed that the reduced ROI will always account for the highest probability of complying with end-point specifications, i.e., the global optimum.

The proposed method has been tested in silico in two well-known case studies to assess its performance. The acetoacetylation of pyrrole with diketene and emulsion polymerization of styrene have been addressed with encouraging results. For both cases, significant levels of intrinsic variability have been added to simulate uncertainty regarding process behavior. It is worth noting that the proposed methodology found an optimal policy with a high probability of success in most cases. As can be expected, because the intrinsic variability is too high, the result obtained gracefully degrades by lowering the probability of success of the optimal policy found.

■ ASSOCIATED CONTENT

Supporting Information

The Supporting Information is available free of charge on the ACS Publications website at DOI: 10.1021/acs.iecr.5b01295.

Detailed first-principles models for the acetoacetylation of pyrrole with diketene and for the emulsion styrene polymerization process, complete sequence of the evolving response surfaces for experimental designs shown in Figure 6, and analysis of the influence of the mixing constant in the methodology (PDF)

■ AUTHOR INFORMATION

Corresponding Author

*E-mail: ecmarti@santafe-conicet.gov.ar. Phone: +54 (342) 4534451. Fax: +54 (342) 4553439.

Notes

The authors declare no competing financial interest.

■ NOMENCLATURE

Symbols

$C_{D,f}$	diketene concentration in the feed stream [mol/L]
C_i	concentration of species i [mol/L]
D_{eff}	D-efficiency of any design ξ with respect to ξ_D*
el	maximum number of external loop iterations
ep	number of designed experimental points in each internal loop
$f(t)$	feed rate [L/min]
il	maximum number of internal loop iterationss
LB/UB	vectors of lower/upper bounds for a given ROI
LB_w/UB_w	low/upper bounds of the input variable w
$\mathbf{M}(\theta,\xi)$	Fisher information matrix
MI	melt flow index [g/min]
MW_n	number-average molecular weight
MW_w	weight-average molecular weight
n	number of points in an experimental design
N_i	total number of particles from population i in the reactor
P_{eff}	P-efficiency of a given design ξ with respect to ξ_P*
q	number of parameters in the response surface model

DOI: 10.1021/acs.iecr.5b01295
Ind. Eng. Chem. Res. XXXX, XXX, XXX−XXX

r	number of replicates to perform in each experimental point
ROI	region of interest for optimization
SP	percentage of variability regarding nominal behavior [%]
t	time [s]
$\mathbf{X}$	matrix data of input variables
x_{des}	designed experimental point
x_k^*	optimal policy from the kth internal loop iteration
x_l^*	optimal policy from the lth external loop iteration

Greek Symbols

α	mixing constant
θ_k	vector of parameters of the response surface model
λ_i^j	jth moment of the live polymer chain for the species i
μ_i^j	jth moment of the dead polymer chain for the species i
$\nu_r(t)$	reactor volume [L]
ε_{in}	stopping criterion for the internal loop
ε_{ex}	stopping criterion for the external loop
ξ	experimental design
ξ_D^*	D-optimal experimental design
ξ_P^*	P-optimal experimental design
$\pi(x_i)$	probability of success for a given operating condition
$\pi(\theta,x)$	response surface model for the probability of success
σ	tensile strength [psi]
$\Phi^{(DP)}$	compound design criterion

REFERENCES

(1) Leal-calderon, F. Emulsified Lipids: Formulation and Control of End-Use Properties. *Ol., Corps Gras, Lipides* **2012**, *19*, 111.

(2) Valappil, J.; Georgakis, C. Nonlinear Model Predictive Control of End-Use Properties in Batch Reactors. *AIChE J.* **2002**, *48*, 2006.

(3) Ferguson, R. M.; Minard, K. R.; Khandhar, A. P.; Krishnan, K. M. Optimizing Magnetite Nanoparticles for Mass Sensitivity in Magnetic Particle Imaging. *Med. Phys.* **2011**, *38*, 1619.

(4) Kolhatkar, A. G.; Jamison, A. C.; Litvinov, D.; Willson, R. C.; Lee, T. R. Tuning the Magnetic Properties of Nanoparticles. *Int. J. Mol. Sci.* **2013**, *14*, 15977.

(5) Paton, K. R.; Varrla, E.; Backes, C.; Smith, R. J.; Khan, U.; O'Neill, A.; Boland, C.; Lotya, M.; Istrate, O. M.; King, P.; et al. Scalable Production of Large Quantities of Defect-Free Few-Layer Graphene by Shear Exfoliation in Liquids. *Nat. Mater.* **2014**, *13*, 624.

(6) Han, J. T.; Jang, J. I.; Kim, H.; Hwang, J. Y.; Yoo, H. K.; Woo, J. S.; Choi, S.; Kim, H. Y.; Jeong, H. J.; Jeong, S. Y.; et al. Extremely Efficient Liquid Exfoliation and Dispersion of Layered Materials by Unusual Acoustic Cavitation. *Sci. Rep.* **2014**, *4*, 5133.

(7) Kong, X.; Yang, Y.; Chen, X.; Shao, Z.; Gao, F. Quality Control via Model-Free Optimization for a Type of Batch Process with a Short Cycle Time and Low Operational Cost. *Ind. Eng. Chem. Res.* **2011**, *50*, 2994.

(8) Zhao, F.; Lu, N.; Lu, J. Quality Control of Batch Processes Using Natural Gradient Based Model-Free Optimization. *Ind. Eng. Chem. Res.* **2014**, *53*, 17419.

(9) Georgakis, C. Design of Dynamic Experiments: A Data-Driven Methodology for the Optimization of Time-Varying Processes. *Ind. Eng. Chem. Res.* **2013**, *52*, 12369.

(10) Martínez, E. C.; Cristaldi, M. D.; Grau, R. J. Dynamic Optimization of Bioreactors Using Probabilistic Tendency Models and Bayesian Active Learning. *Comput. Chem. Eng.* **2013**, *49*, 37.

(11) Luna, M.; Martínez, E. A Bayesian Approach to Run-to-Run Optimization of Animal Cell Bioreactors Using Probabilistic Tendency Models. *Ind. Eng. Chem. Res.* **2014**, *53*, 17252.

(12) Luna, M. F.; Martinez, E. C. Run-to-Run Optimization of Biodiesel Production Using Probabilistic Tendency Models - A Simulation Study. *Can. J. Chem. Eng.* **2015**, *93*, 1613.

(13) Anand, F. S.; Lee, J. H.; Realff, M. J. Optimal Decision-Oriented Bayesian Design of Experiments. *J. Process Control* **2010**, *20*, 1084.

(14) Marchetti, A.; Chachuat, B.; Bonvin, D. Modifier-Adaptation Methodology for Real-Time Optimization. *Ind. Eng. Chem. Res.* **2009**, *48*, 6022.

(15) Mandur, J. S.; Budman, H. M. Simultaneous Model Identification and Optimization in Presence of Model-Plant Mismatch. *Chem. Eng. Sci.* **2015**, *129*, 106.

(16) Fiordalis, A.; Georgakis, C. Data-Driven, Using Design of Dynamic Experiments, versus Model-Driven Optimization of Batch Crystallization Processes. *J. Process Control* **2013**, *23*, 179.

(17) McGree, J. M.; Eccleston, J. A.; Duffull, S. B. Compound Optimal Design Criteria for Nonlinear Models. *J. Biopharm. Stat.* **2008**, *18*, 646.

(18) McGree, J. M.; Eccleston, J. A. Probability-Based Optimal Design. *Aust. N. Z. J. Stat.* **2008**, *50*, 13.

(19) Woods, D. C.; Lewis, S. M.; Eccleston, J. A.; Russell, K. G. Designs for Generalized Linear Models with Several Variables and Model Uncertainty. *Technometrics* **2006**, *48*, 284.

(20) McCullagh, P. Generalized Linear Models. *Eur. J. Oper. Res.* **1984**, *16*, 285.

(21) Nelder, J. A.; Wedderburn, R. W. M. Generalized Linear Models. *J. R. Stat. Soc.* **1972**, *135*, 370.

(22) Montgomery, D. C.; Runger, G. C. *Applied Statistics and Probability for Engineers*, 3rd ed.; John Wiley & Sons, Inc.: New York, 2002.

(23) Ruppen, D.; Bonvin, D.; Rippin, D. W. T. Implementation of Adaptive Optimal Operation for a Semi-Batch Reaction System. *Comput. Chem. Eng.* **1998**, *22*, 185.

(24) Liotta, V.; Georgakis, C.; Sudol, E. D.; El-Aasser, M. S. Manipulation of Competitive Growth for Particle Size Control in Emulsion Polymerization. *Ind. Eng. Chem. Res.* **1997**, *36*, 3252.

(25) Li, B.-G.; Brooks, B. W. Prediction of the Average Number of Radicals per Particle for Emulsion Polymerization. *J. Polym. Sci., Part A: Polym. Chem.* **1993**, *31*, 2397.

(26) Liotta, V.; Sudol, E. D.; El-Aasser, M. S.; Georgakis, C. On-Line Monitoring, Modeling, and Model Validation of Semibatch Emulsion Polymerization in an Automated Reactor Control Facility. *J. Polym. Sci., Part A: Polym. Chem.* **1998**, *36*, 1553.

(27) Crowley, T. J.; Choi, K. Y. Calculation of Molecular Weight Distribution from Molecular Weight Moments in Free Radical Polymerization. *Ind. Eng. Chem. Res.* **1997**, *36*, 1419.

(28) Meyer, T.; Keurentjes, J. *Handbook of Polymer Reaction Engineering*; Wiley-VCH Verlag GmbH: Weinheim, Germany, 2005; p 1.

(29) Katz, S.; Saidel, G. M. Moments of the Size Distribution in Radical Polymerization. *AIChE J.* **1967**, *13*, 319.

DOI: 10.1021/acs.iecr.5b01295
Ind. Eng. Chem. Res. XXXX, XXX, XXX−XXX